RM L54K16a

NACA

RESEARCH MEMORANDUM

EFFECTS OF AN INSET TAB ON THE HINGE-MOMENT AND EFFECTIVENESS CHARACTERISTICS OF AN UNSWEPT TRAILING-EDGE CONTROL ON A 60° DELTA WING AT MACH NUMBERS FROM 0.75 TO 1.96

By Lawrence D. Guy and Hoyt V. Brown

Langley Aeronautical Laboratory
Langley Field, Va.

NATIONAL ADVISORY COMMITTEE FOR AERONAUTICS

WASHINGTON

February 15, 1955
Declassified March 13, 1959

NATIONAL ADVISORY COMMITTEE FOR AERONAUTICS

RESEARCH MEMORANDUM

EFFECTS OF AN INSET TAB ON THE HINGE-MOMENT AND EFFECTIVENESS CHARACTERISTICS OF AN UNSWEPT TRAILING-EDGE CONTROL ON A 60° DELTA WING AT MACH NUMBERS FROM 0.75 TO 1.96

By Lawrence D. Guy and Hoyt V. Brown

SUMMARY

An investigation of the effects of an inset tab on the hinge-moment and effectiveness characteristics of an unswept trailing-edge control on a 60° delta wing has been made in the Langley 9- by 12-inch blowdown tunnel at Mach numbers of 0.75 to 1.96. Rolling-moment and lift effectiveness of the tab-flap combination as well as control hinge moments were obtained over a large range of tab and flap deflections for angles of attack up to 12°.

The results indicated that ratios of tab to flap deflections required for zero hinge moments due to control deflections increased in magnitude from -0.5 to -2.0 as speed was increased in the transonic speed range and were nearly constant at Mach numbers above 1.25. One-hundred-percent balance of the flap hinge moments due to deflection was limited to flap deflections only slightly greater than 10° up and down because of reduced balancing effectiveness of the tab at large deflections. However, at 20° flap deflection the tab was still capable of balancing at least 50 percent of the flap hinge moments. The rolling-moment effectiveness of the tab-flap combination deflected for zero flap hinge moment due to deflection decreased from about 80 percent to 50 percent of that for the flap with the tab undeflected as the Mach number increased from 0.75 to 1.96.

For the conditions of equal rolling moment, theoretical calculations at supersonic speeds indicate that, with the flap free on its hinge axis, deflection of the tab required about 19 percent of the hinge moment and 60 to 75 percent of the deflection work required for deflection of an untabbed flap of the same overall dimension.

INTRODUCTION

Aerodynamic balancing of control hinge moments has become increasingly important as the speed of aircraft and missiles has increased, both to reduce the power and size of boost systems and control-actuating mechanisms and to provide positive control in the event of power failure. Balancing tabs have long been used at subsonic speeds to reduce control hinge moments, and theoretical and experimental investigations (refs. 1 and 2) have shown that trailing-edge flap-tab combinations, by proper choice of flap-tab deflection ratios, could give nearly complete hinge-moment balance at subsonic speeds with relatively high lift effectiveness. Although the limited information available (for example, refs. 3 to 5) indicates that such a balance arrangement loses many of its advantages when supersonic speeds are reached, it is desirable to obtain more information on this type of balance at both transonic and supersonic speeds. In order to furnish such information an investigation has been made in the Langley 9- by 12-inch blowdown tunnel on a 60° delta wing with a trailing-edge flap equipped with an inset tab at Mach numbers of 0.75 to 1.96.

The aerodynamic characteristics of the complete semispan model as well as hinge moments of the flap-tab combination were obtained over an angle-of-attack range of ±12°, a flap-deflection range of 0° to 20°, and a tab-deflection range of 0° to -40°. The tests were made in three supersonic nozzles at Mach numbers of 1.41, 1.62, and 1.96 and Reynolds numbers of 2.9×10^6, 2.7×10^6, and 2.5×10^6, respectively. Tests were also made in a transonic nozzle at Mach numbers of 0.75 to 1.25 and Reynolds numbers of 2.8×10^6 to 3.3×10^6.

COEFFICIENTS AND SYMBOLS

C_L lift coefficient, $\frac{\text{Lift}}{qS}$

$C_{l_{gross}}$ gross rolling-moment coefficient (reference axis shown in fig. 1), $\frac{\text{Semispan-model rolling moment}}{2qSb}$

C_h control hinge-moment coefficient, $\frac{H}{qb_f\bar{c}_f^2}$

C_{h_t} tab hinge-moment coefficient, $\frac{H_t}{qb_f\bar{c}_f^2}$

$C_l, \Delta C_L, \Delta C_h$ increment in gross rolling-moment, lift, and hinge-moment coefficient due to deflection of either flap or tab, or both

H hinge moment about flap hinge line, in-lb

H_t hinge moment about tab hinge line, in-lb

w_t tab deflection work, $b_f \bar{c}_f^2 q \left[\int_0^{\delta_t} C_{h_t} \, d\left(\frac{\delta_t}{57.3}\right) \right]$, in-lb

w_{fu} flap deflection work, $b_f \bar{c}_f^2 q \left[\int_0^{\delta_{fu}} C_{h_{fu}} \, d\left(\frac{\delta_{fu}}{57.3}\right) \right]$, in-lb

$$\frac{dC_{h_t}}{d\delta_f} = \left(\frac{\partial C_{h_t}}{\partial \delta_f} + \frac{\partial C_{h_t}}{\partial \delta_t} \frac{\delta_t}{\delta_f} \right)_{\alpha=\text{Constant}}$$

S semispan wing area (including area blanketed by test body), in.

c local wing chord, in.

$\bar{c}$ mean aerodynamic chord of wing, in.

b wing span, twice distance from the rolling-moment reference axis to wing tip, in.

b_f flap span, in.

$\bar{c}_f$ mean aerodynamic chord of flap rearward of hinge line, in.

α wing angle of attack, deg

δ_f flap deflection relative to wing chord plane (positive when flap trailing edge is down), deg

δ_t tab deflection relative to flap chord plane (positive when tab trailing edge is down), deg

M free-stream Mach number

q free-stream dynamic pressure, lb/sq in.

R Reynolds number based on mean aerodynamic chord of wing

Subscripts:

α slope of curve of coefficient plotted against α: $\frac{\partial C_h}{\partial \alpha}$, $\frac{\partial C_L}{\partial \alpha}$, and so forth

δ slope of curve of coefficient plotted against δ: $\frac{\partial C_h}{\partial \delta}$, $\frac{\partial C_l}{\partial \delta}$, and so forth

f tabbed flap

fu untabbed flap

t tab

DESCRIPTION OF MODEL

The principal dimensions of the semispan wing-fuselage combination are shown in figure 1 and a photograph of the model is shown in figure 2. The wing was of delta plan form having 60° leading-edge sweepback and a corresponding aspect ratio of 2.3. A constant-chord, 40-percent-semispan control was located at the wing trailing edge with the control inboard end at $0.30b/2$.

The main wing panel, exclusive of the control surface, was made of stainless steel and had 4-percent-thick modified hexagonal airfoil sections. The leading edge was modified by a small nose radius as shown in figure 1. The trailing-edge thickness tapered from 0.01 inch at the outboard end of the flap to 0.002 inch at the wing tip and was constant at 0.01 inch inboard of the flap. Inboard of the control surface, the wing thickness was increased to 2.95 percent along the ray shown in figure 1 to permit installation of an internal torque rod for use with a strain-gage beam inside the test body.

The constant-chord control was machined from mild steel. A groove machined on both sides of the control at 71 percent of the control chord permitted the remaining 29 percent of the control to be deflected as an inset tab. This groove was filled with cement to eliminate a break in contour for all tests. The outboard end of the control was hinged by a 0.040-inch-diameter pin to the main wing panel. At the inboard end a 0.095-inch-diameter shaft, integral with the control, extended through the wing to a bearing and a clamp which were part of an electrical strain-gage beam contained within the test body.

A fuselage consisting of a half body of revolution mounted on a 0.25-inch shim was attached to the wing for all tests. The bottom portion of the shim was insulated from the rest of the model and permitted an electrical indication of model fouling.

TUNNEL

The tests were conducted in the Langley 9- by 12-inch blowdown tunnel which utilizes the air of the Langley 19-foot pressure tunnel. The absolute stagnation pressure of the air entering the test section ranges from 2 to $2\frac{1}{3}$ atmospheres. The compressed air is conditioned to insure condensation-free flow in the test section by being passed through a silica-gel drier and then through banks of finned electrical heaters. Criteria for condensation-free flow were obtained from reference 6. Turbulence damping screens are located in the settling chamber. Four interchangeable nozzle blocks provide test-section Mach numbers of 0.71 to 1.30, 1.41, 1.62, and 1.96.

Supersonic nozzles.- Test-section flow conditions of the three supersonic nozzles with the tunnel clear were determined from extensive calibration measurements and schlieren photographs and reported in reference 7. Deviations of flow conditions in the test section are listed below:

	M = 1.41	M = 1.62	M = 1.96
Maximum deviation in Mach number	±0.002	±0.01	±0.02
Maximum deviation in stream angle, deg . .	±0.25	±0.20	±0.20
Reynolds number (approx.)	2.9×10^6	2.7×10^6	2.5×10^6

Transonic nozzle.- A description of the transonic nozzle, which has a 7- by 10-inch test section, together with a discussion of the flow characteristics obtained from limited calibration tests, is presented in reference 8. Satisfactory test-section flow characteristics are indicated from the minimum Mach number ($M \approx 0.7$) to about $M = 1.20$. The maximum deviations from the average Mach number in the region occupied by the model are shown in figure 3. Stream angle deviation probably did not exceed $\pm 0.1^\circ$ at any Mach number. The variation with Mach number of the average test Reynolds number is also given in figure 3 together with the approximate limits of the variation during the tests.

TEST TECHNIQUE

The semispan model was cantilevered from a five-component strain-gage balance mounted flush with the tunnel floor. The balance and model

rotated together as the angle of attack was changed and the aerodynamic moments and forces on the wing were measured with respect to the balance axis and then rotated to the wind axis. The control-surface hinge moments were measured by means of a strain-gage beam contained within the test body. The test body consisted of a half body of revolution mounted on a 0.25-inch shim; the shim was used to minimize wall-boundary-layer effects (refs. 9 and 10). A clearance gap of 0.01 to 0.02 inch was maintained between the fuselage shim and the tunnel floor.

CORRECTIONS

No corrections are available to allow for jet-boundary interference and blockage or for reflection-plane effects at high subsonic speeds. Further, reflection by the tunnel walls of the model shock and expansion waves back on to the model may appreciably affect the model loadings due to angle of attack at small supersonic Mach numbers but should not appreciably affect the loading due to control deflection. Comparisons of experimental results obtained in the blowdown tunnel with those obtained in other facilities (ref. 8), however, are evincive of the reliability of wing and control characteristics due to angle of attack obtained at high subsonic speeds and of control characteristics due to control deflection obtained throughout the Mach number range from 0.7 to 1.2. For further discussion, see reference 8.

ACCURACY OF DATA

An estimate has been made of the probable errors to be found in the measured values due to calibration, measuring equipment, and instrument reading errors and are presented in the following table:

	Error
α, deg	± 0.05
δ_f, deg	± 0.2
δ_t, deg	± 0.4
C_L	± 0.01
C_l	± 0.001
C_h	± 0.008

The errors in δ_f and δ_t above are the errors in no-load control settings. Corrections have been applied to the data for the additional variation in flap deflection due to control loading.

The present investigation was made before the calibration of the transonic nozzle had been completed. The calibration from which the Mach number and dynamic pressure was determined was made with a pressure probe which was less accurate than desirable. Further, this calibration was referenced to the ratio of static pressure at an orifice in the tunnel wall to the settling-chamber pressure, and subsequent tests have shown that the pressure measured at this wall orifice was unduly influenced by the model. Errors in measured pressures introduced by these factors caused errors in the indicated Mach numbers of as much as 0.03 and resulted in errors in dynamic pressure which caused the value of the data coefficients to be from 2.0 to 3.5 percent too high at transonic Mach numbers. The data have been plotted at the correct Mach number.

RESULTS AND DISCUSSION

Hinge-moment, lift, and rolling-moment coefficients of the semispan-wing—fuselage combination plotted against angle of attack for various flap and tab deflections at $M = 1.96$ are presented in figure 4. These data are representative of those obtained at other Mach numbers and indicate the quality of the data obtained in this investigation. Figure 5 presents the variation of hinge-moment coefficient and rolling-moment coefficient with flap deflection for $\alpha = \delta_t = 0^\circ$ and the variation of hinge-moment coefficient with angle of attack for $\delta_f = \delta_t = 0^\circ$ at various Mach numbers. Rolling-moment coefficient and the increment in hinge-moment coefficient due to tab deflection is plotted against tab deflection in figure 6 for various flap deflections and Mach numbers at zero angle of attack. In figure 7 and subsequent figures data are shown at negative flap deflections for convenience of presentation. These data were obtained from negative angle-of-attack data by arbitrarily reversing the signs of test values of angle of attack, flap and tab deflections, and model force and moment coefficients. This was permissible by reason of model symmetry.

Control hinge moments.- The ratios of tab deflection to flap deflection shown in figure 7 indicate the tab deflection required for 100-percent balance of the hinge moments due to flap deflections of $\pm 5^\circ$ and $\pm 10^\circ$. In practice important reductions in the overall force needed for control deflection could be obtained with arrangements yielding less than complete balance of the flap hinge moments. However, the ratios of δ_t/δ_f for $\Delta C_h = 0$ provide a convenient parameter for comparison of the tab balancing effectiveness at various Mach numbers.

For a flap deflection of $\pm 5^\circ$ the δ_t/δ_f ratios, in general, increased with Mach number from a value of about -0.5 at the lowest Mach number to a maximum value of about -2 at $M = 1.25$ and then remained essentially constant with further increase in Mach number (fig. 7). The δ_t/δ_f ratios

for -10° flap deflection were larger than those for -5° flap deflection by an almost constant increment through the angle-of-attack range for a given Mach number. However, for positive flap deflections this same increment was evident at $\alpha = 0^\circ$ but decreased with increasing angle of attack at Mach numbers above $M = 0.9$.

Figure 5 (as well as fig. 12) shows that the rapid increases in δ_t/δ_f ratios with Mach number were primarily due to the increase in slope of C_h against δ_f which was associated with the rearward shift in the control center of pressure in the transonic speed range. In figure 6 the hinge moment due to tab deflection showed no such increase in the transonic range (see also fig. 12) probably because the narrow tab chord did not permit an appreciable change in the length of the moment arm of the tab loading due to center-of-pressure shift.

The increases in values of δ_t/δ_f required by an increase in magnitude of δ_f (fig. 7) are explained by reference to figure 6. These data showed that the hinge moments per unit tab deflection $\left(C_{h_{\delta_t}}\right)$ decreased with an increase in tab deflection and to some extent with an increase in flap deflection. Consequently, larger values of δ_t/δ_f were required to balance out the control hinge moments as flap deflection was increased. At subsonic speeds, for flap deflections up to 10°, the hinge-moment coefficients required of the tab for balance intersected the steep portion of the curves and values of δ_t/δ_f increased only slightly. However, as the hinge moments required of the tab increased with Mach number, they intersected higher on the curves where the slope decreased rapidly and values of δ_t/δ_f increased correspondingly. The decrease in δ_t/δ_f with an increase in angle of attack that is shown for 10° flap deflection at supersonic speeds resulted from only small changes in $C_{h_{\delta_f}}$ and $C_{h_{\delta_t}}$ with increased angle of attack.

It appears from the above considerations that at supersonic speeds the tab would be incapable of completely balancing out the flap hinge moments due to deflection for flap deflections much above 10°. If, however, less than 100-percent balance was desired, the useful range of the tab would be increased correspondingly; that is, since $C_{h_{\delta_f}}$ does not increase with increasing deflection (fig. 5), the tab is capable of balancing at least 50 percent of the hinge moments due to 20° flap deflection with tab deflections no greater than those required for 100-percent balance of 10° flap deflection (fig. 7).

Figure 8 indicates the variation with Mach number of the tab deflection required to balance out the total control hinge moments due to the

combination of both control deflection and angle of attack. These data indicate that at angles of attack of 4° and 8° the tab was incapable of balancing out the total control hinge moments for flap deflections of 10° or larger except at Mach numbers less than 0.86. Further, at Mach numbers above 0.86 the δ_t/δ_f ratios required for 5° flap deflection increased rapidly with angle of attack and quickly became too large for the tab to be of practical use in balancing out the total hinge moments. Also shown in figure 8 are ratios of δ_t/α which indicate the tab deflection required to balance the hinge moments due to the control angle-of-attack loading ($\delta_f = 0^\circ$).

Control effectiveness.- The variation with Mach number of the rolling-moment coefficient due to flap and tab deflection for $\Delta C_h = 0$ is shown in figure 9. These data show that the rolling-moment effectiveness of the flap-tab combination decreased rapidly with increasing Mach number in the transonic speed range, then less rapidly at supersonic speeds. The reduction in C_l at zero angle of attack was about 70 percent between $M = 0.86$ and $M = 1.25$ for 5° flap deflection. The rate of decrease in C_l with Mach number corresponded roughly to the rate of increase of the ratios of δ_t/δ_f with Mach number (fig. 7) since the variation of C_l with δ_f and δ_t was generally linear for the angle condition of the tests. This does not mean, however, that the decrease in C_l for $\Delta C_h = 0$ is entirely due to tab deflection since the roll effectiveness of plain trailing-edge flap-type controls also decreases in the transonic range (see also fig. 13). To show the loss in control effectiveness due to tab deflection, the ratios of C_l for $\Delta C_h = 0$ to C_l for $\delta_t = 0^\circ$ are plotted against Mach number in figure 10. For 5° flap deflection the rolling moment of the flap-tab combination was generally about 80 percent of that of the untabbed flap at the lowest Mach number and about 50 percent of the untabbed flap at the highest Mach number. For 10° flap deflection the ratios were generally about 10 percent lower, except at subsonic Mach numbers where the difference was less.

Figure 11 presents the lift increment of the flap-tab combination for a zero hinge moment due to both control deflection and angle of attack. Also shown are the decrements in lift coefficient due to the tab deflection required to balance C_h due to $\alpha(\delta_f = 0)$. The large tab deflections required to balance out the total control hinge moment (fig. 8) plus the very small increments in lift resulting from flap and tab deflections indicate that the inset tab would be an inadequate balance for this type of flap when used as a longitudinal control at supersonic speeds.

Comparison of experiment with theory.- Figures 12 and 13 present comparisons of experimental with theoretical values of some control hinge-moment and effectiveness parameters at supersonic speeds. All hinge-moment

coefficients are based on the moment area of all the control surface behind the flap hinge line, including tab, to allow direct comparison of the flap and tab hinge moments. The angle conditions given in figure 12 indicate the range over which the experimental slope parameters were obtained. Theoretical loadings due to control-surface deflection were obtained from equations of reference 11 and loading due to angle of attack from equations in the appendix of reference 8. In figure 12 values of δ_t/δ_f were obtained directly from the given values of $C_{h_{\delta_t}}$ and $C_{h_{\delta_f}}$ by the equation $\frac{\delta_t}{\delta_f} = \frac{C_{h_{\delta_f}}}{C_{h_{\delta_t}}}$.

Figure 12 shows that above $M = 1.4$ the experimental values of C_{h_α} and $C_{h_{\delta_f}}$ were 75 to 80 percent of the theoretical values, whereas experimental values of $C_{h_{\delta_t}}$ were only 60 to 75 percent of the theoretical values. Although, as a consequence, theory underestimates the experimental values of δ_t/δ_f, the prediction is within about 15 percent of experiment.

Sizable differences are shown in figure 13 between experimental and theoretical values of the rolling-moment effectiveness parameters $C_{l_{\delta_f}}$ and $C_{l_{\delta_t}}$, with experiment being less than 50 percent of the prediction in the case of $C_{l_{\delta_t}}$. The effectiveness of the flap-tab combination deflected for $\Delta C_h = 0$, however, agreed well with theory. As a consequence of this variance, the ratios of $C_{l_{\delta_f}}$ for the control with the tab deflected for $\Delta C_h = 0$ to that for the tab undeflected were from 10 to 20 percent greater than the theoretical prediction. It should be noted that in the case of $C_{l_{\delta_t}}$ the differences between theory and experiment are of the same order as the experimental accuracy at the highest Mach numbers.

The theoretical calculations have been extended in order to aid in the evaluation of the characteristics of the tabbed flap relative to those of an untabbed flap and are shown in figure 14. The top curve in figure 14 indicates that deflection of the tab to balance the flap hinge moments would result in tab hinge moments per unit flap deflection being less than 10 percent of those for the flap without the tab (theoretical values of $C_{h_{\delta_f}}$ in fig. 12). However, theory (fig. 13) indicates that the rolling-moment effectiveness of the tabbed flap relative to the

untabbed flap would be reduced by about 50 percent. If it is required that the rolling moments for the tabbed flap and the untabbed flap be equal, theory indicates that tab hinge moments with the tab deflected for $\Delta C_h = 0$ would be about 19 percent of the untabbed-flap hinge moments (fig. 14). Inasmuch as previous comparisons showed that theory tends to overestimate the tab hinge moments while underestimating the relative rolling-moment effectiveness of the tabbed and untabbed flap, the true picture appears to be even brighter. In any case, it is evident that substantial reductions in strength and weight of the control-actuating mechanisms could be expected.

Another important consideration is the work required to overcome the hinge moments due to deflection for the reason that it determines the amount of energy that must be supplied to the control system. The lower curve of figure 14 indicates that the deflection work required to deflect the tab of the tab-flap combination would be 60 to 75 percent of the work required to deflect an untabbed flap providing the same rolling moment. For some applications this saving in energy could be very important particularly in this speed range. It must be kept in mind, however, that, although the theoretical predictions appear to be conservative, they are applicable only to small angle conditions and that the experimental data have shown limitations on the usable flap and tab deflection range.

SUMMARY OF RESULTS

An investigation was made at Mach numbers from 0.75 to 1.96 in the Langley 9- by 12-inch blowdown tunnel to determine the balancing effects of an inset tab on a trailing-edge flap-type control mounted on a 60° delta wing. The following results were indicated for angles of attack up to 8°:

1. The ratio of the tab to flap deflection required to balance out completely the hinge moments due to ±5° flap deflection increased from -0.5 to -2.0 in the transonic speed range and was nearly constant for Mach numbers from 1.25 to 1.96. Complete balance of the flap hinge moments due to deflection could not be obtained at flap deflections much above 10° because of reduced balancing effectiveness of the tab at large deflections. However, at 20° flap deflection the tab was capable of balancing at least 50 percent of the flap hinge moments.

2. The rolling-moment effectiveness of the flap-tab combination deflected for zero flap hinge moments due to deflection decreased from about 80 percent to 50 percent of that for the flap alone as the Mach number increased from 0.75 to 1.96.

3. Theoretical calculations at supersonic speeds indicated that, for conditions of equal rolling moment, deflecting the inset tab for zero flap

hinge moments would require about 19 percent of the force and 60 to 75 percent of the deflection work as deflecting an untabbed flap of the same overall dimension (at zero angle of attack).

Langley Aeronautical Laboratory,
National Advisory Committee for Aeronautics,
Langley Field, Va., Nov. 2, 1954.

REFERENCES

1. Sears, Richard I.: Wind-Tunnel Data on the Aerodynamic Characteristics of Airplane Control Surfaces. NACA WR L-663, 1943. (Formerly NACA ACR 3L08.)

2. Spearman, M. Leroy: Wind-Tunnel Investigation of Control-Surface Characteristics. XXIII - A 0.25-Airfoil-Chord Flap With Tab Having a Chord Twice the Flap Chord of an NACA 0009 Airfoil. NACA WR L-47, 1945. (Formerly NACA ARR L5G25.)

3. Lockwood, Vernard E., and Fikes, Joseph E.: Preliminary Investigation at Transonic Speeds of the Effect of Balancing Tabs on the Hinge-Moment and Other Aerodynamic Characteristics of a Full-Span Flap on a Tapered 45° Sweptback Wing of Aspect Ratio 3. NACA RM L52A23, 1952.

4. Bland, William M., Jr., and Marley, Edward T.: A Free-Flight Investigation at Zero Lift in the Mach Number Range Between 0.7 and 1.4 To Determine the Effectiveness of an Inset Tab as a Means of Aerodynamically Relieving Aileron Hinge Moments. NACA RM L52K07, 1952.

5. Boyd, John W., and Pfyl, Frank A.: Experimental Investigation of Aerodynamically Balanced Trailing-Edge Control Surfaces on an Aspect Ratio 2 Triangular Wing at Subsonic and Supersonic Speeds. NACA RM A52L04, 1953.

6. Burgess, Warren C., Jr., and Seashore, Ferris L.: Criterions for Condensation-Free Flow in Supersonic Tunnels. NACA TN 2518, 1951.

7. May, Ellery B., Jr.: Investigation of the Effects of Leading-Edge Chord-Extensions on the Aerodynamic and Control Characteristics of Two Sweptback Wings at Mach Numbers of 1.41, 1.62, and 1.96. NACA RM L50L06a, 1951.

8. Guy, Lawrence D.: Effects of Overhang Balance on the Hinge-Moment and Effectiveness Characteristics of an Unswept Trailing-Edge Control on a 60° Delta Wing at Transonic and Supersonic Speeds. NACA RM L54G12a, 1954.

9. Conner, D. William: Aerodynamic Characteristics of Two All-Movable Wings Tested in the Presence of a Fuselage at a Mach Number of 1.9. NACA RM L8H04, 1948.

10. Mitchell, Meade H., Jr.: Effects of Varying the Size and Location of Trailing-Edge Flap-Type Controls on the Aerodynamic Characteristics of an Unswept Wing at a Mach Number of 1.9. NACA RM L50F08, 1950.

11. Goin, Kennith L.: Equations and Charts for the Rapid Estimation of Hinge-Moment and Effectiveness Parameters for Trailing-Edge Controls Having Leading and Trailing Edges Swept Ahead of the Mach Lines. NACA Rep. 1041, 1951. (Supersedes NACA TN 2221.)

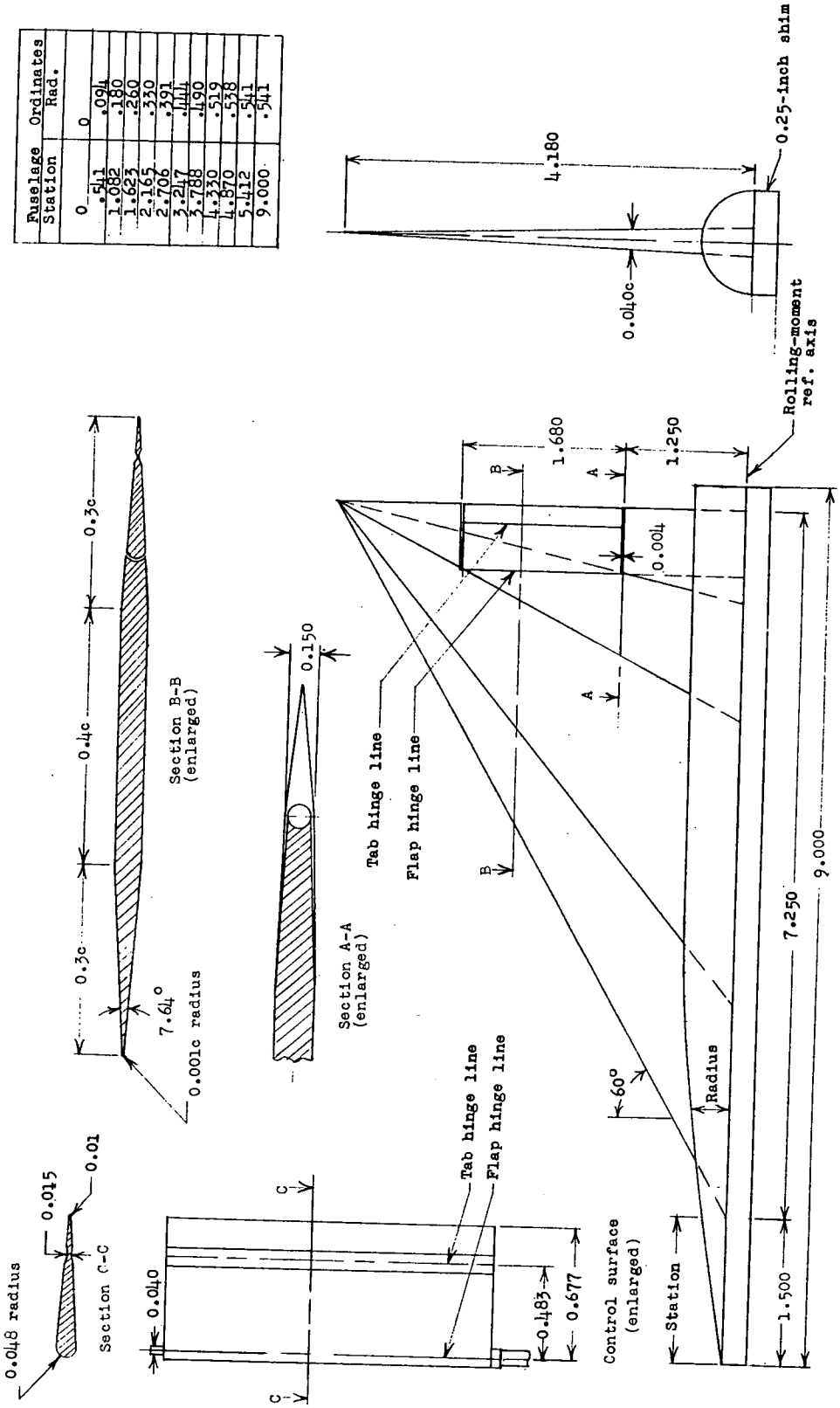

Figure 1.- Details of 60° sweptback wing, fuselage, and control. Wing area, 15.153 sq in.; flap area, 1.132 sq in.; tab area, 0.324 sq in.; M.A.C., 4.833 in. All dimensions are in inches.

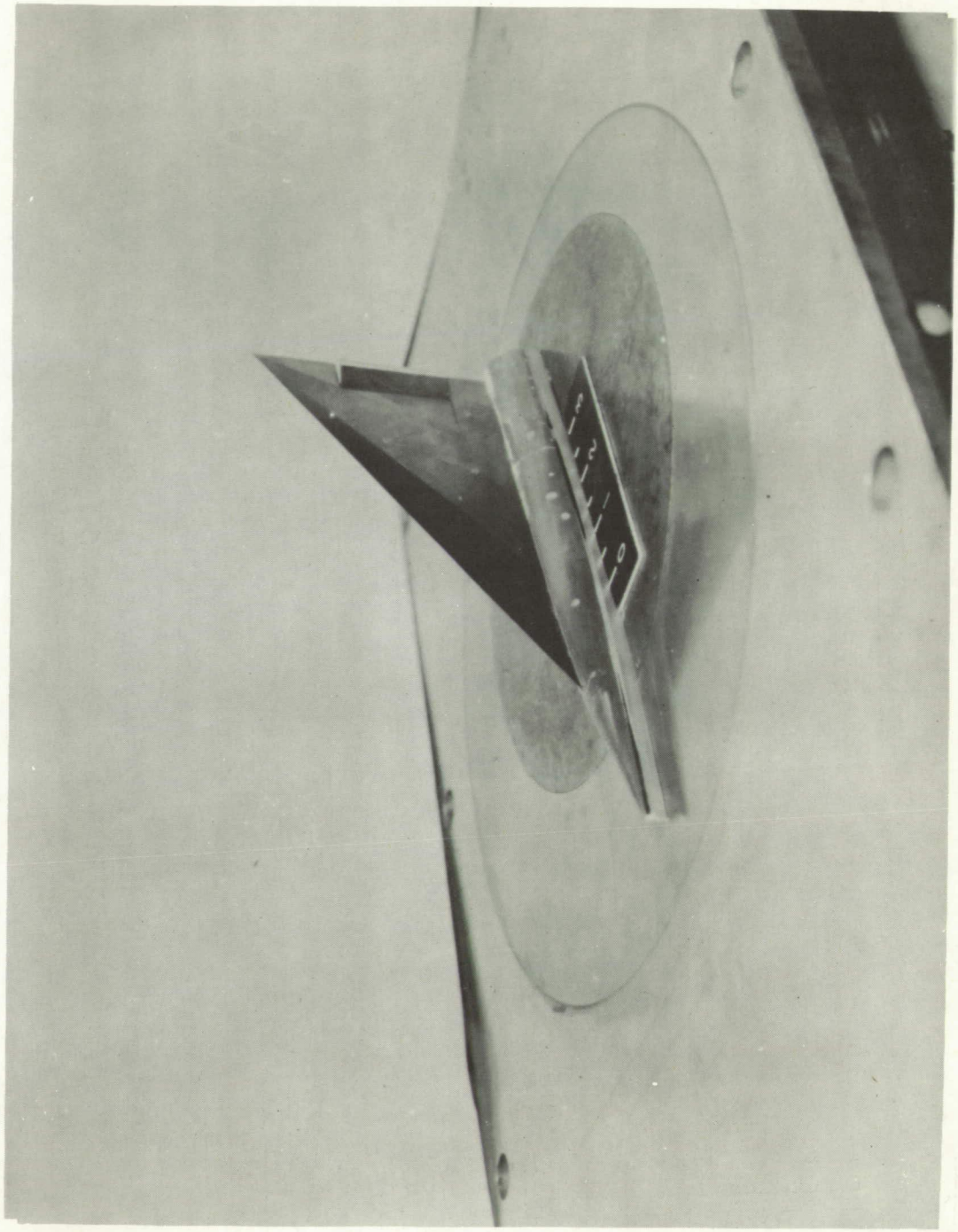

L-80536

Figure 2.- Photograph of model.

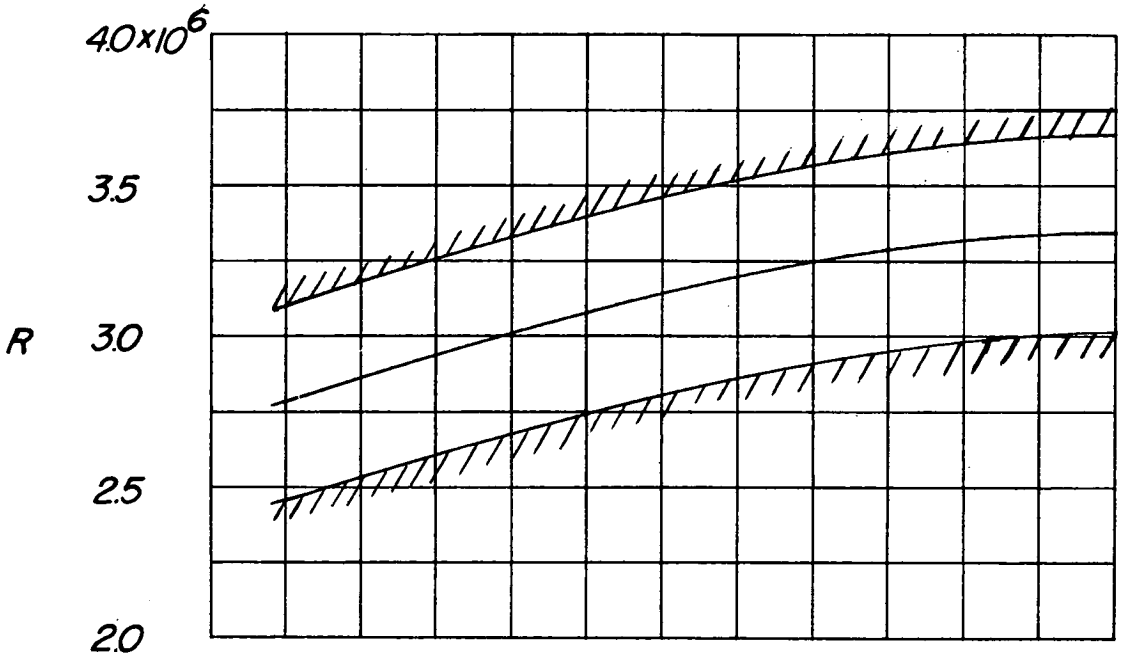

(a) Test Reynolds number based on $\bar{c}$ of 60° delta wing.

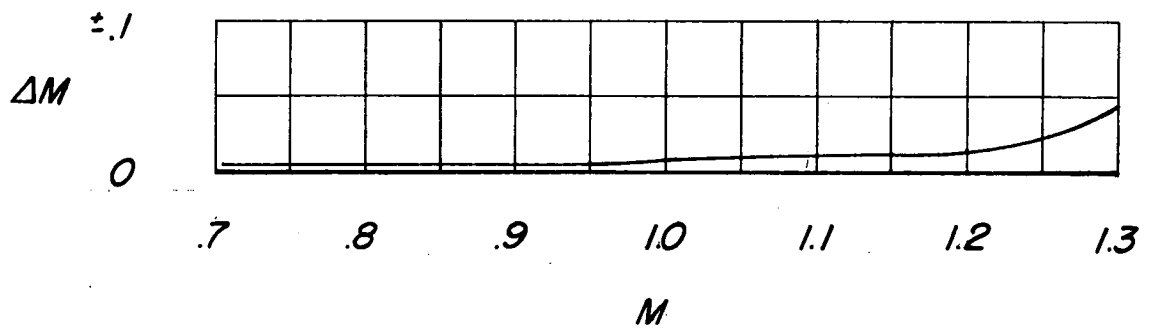

(b) Maximum deviation from average test-section Mach number.

Figure 3.- Test-section Mach number and Reynolds number characteristics of the transonic nozzle.

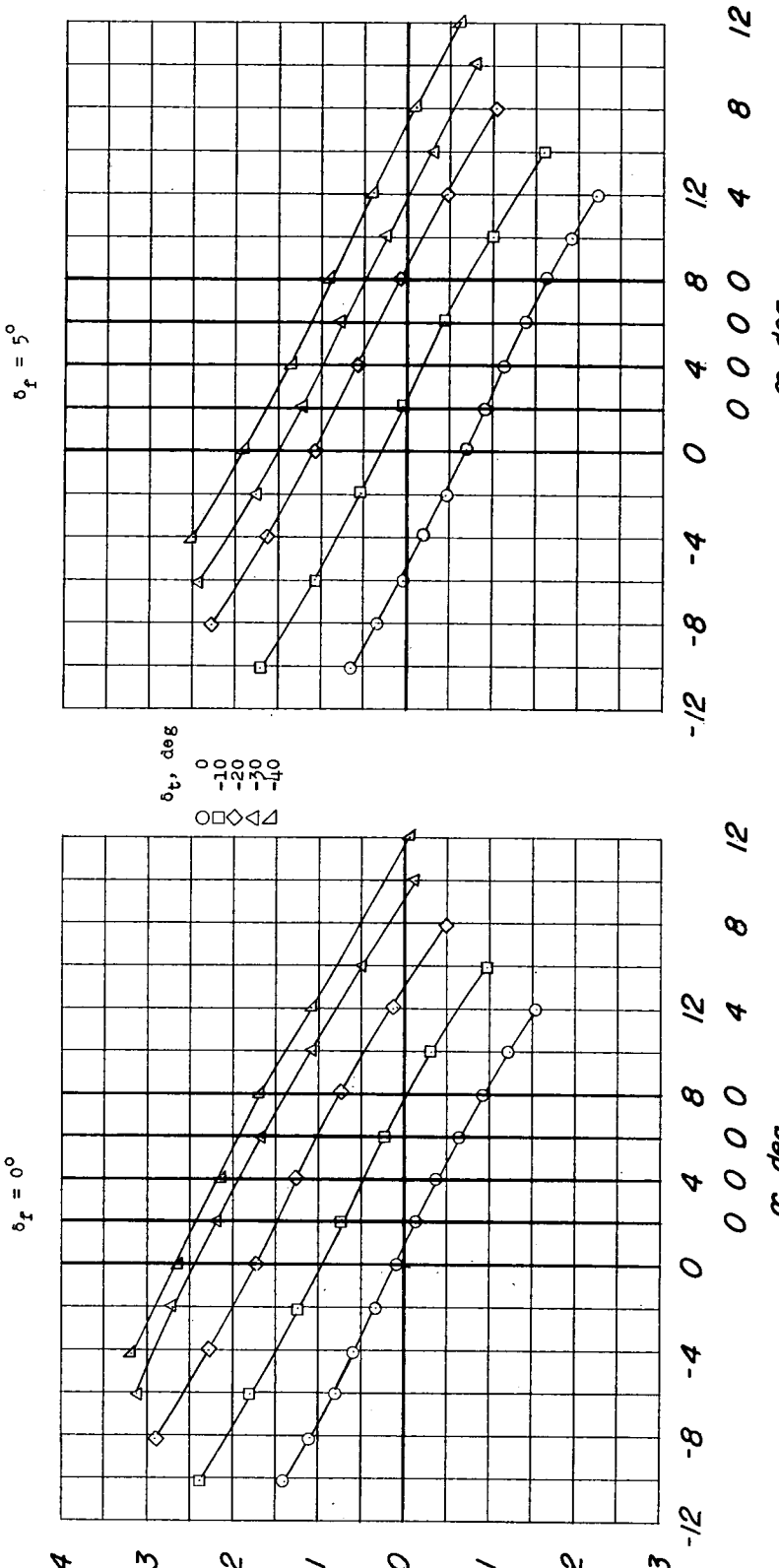

(a) C_h against α.

Figure 4.- Aerodynamic characteristics of a semispan-delta-wing—fuselage combination with a constant-chord, trailing-edge control equipped with an inset tab. R = 2.5 × 10⁶; M = 1.96.

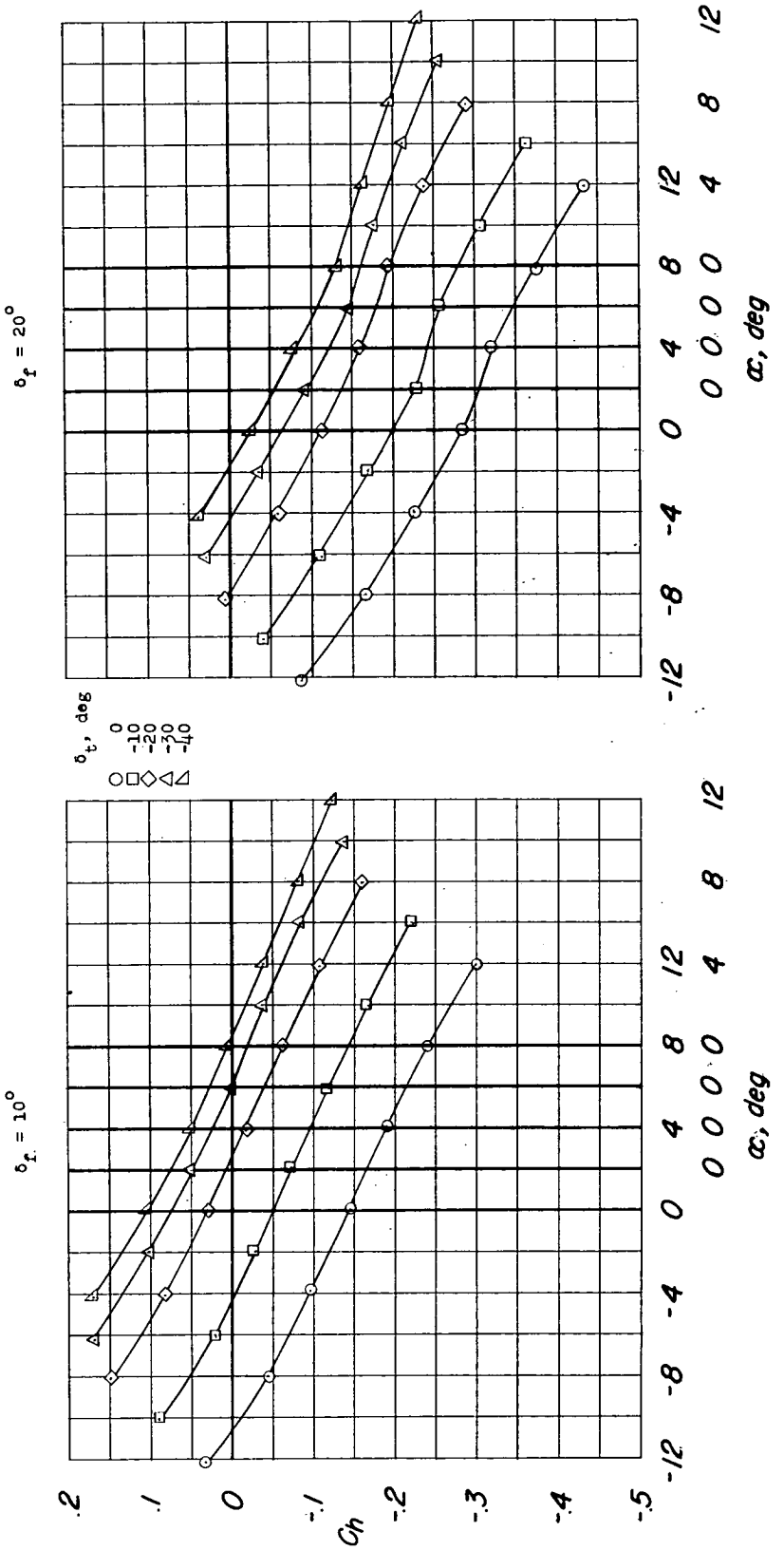

(a) Concluded.

Figure 4.- Continued.

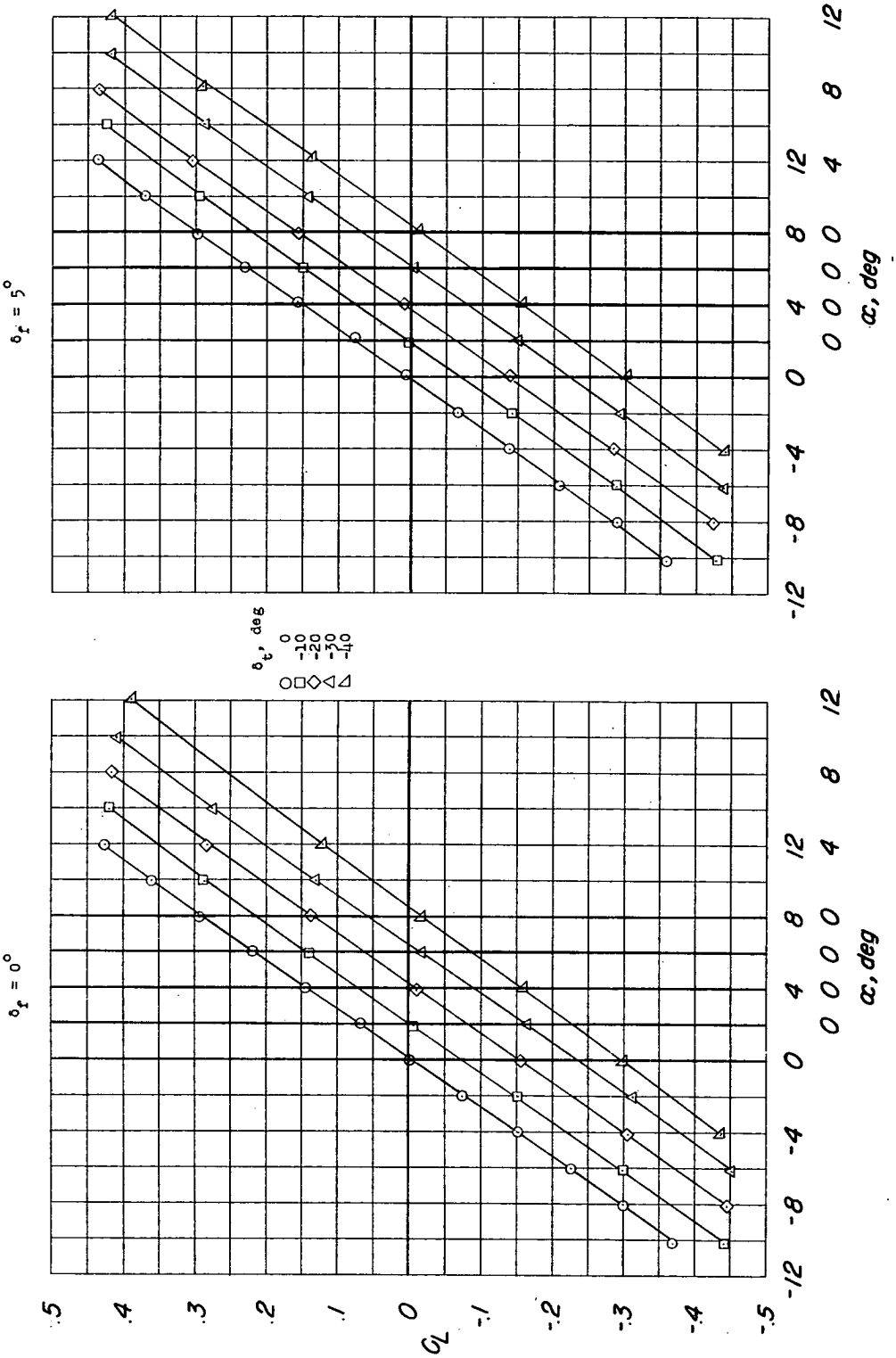

(b) C_L against α.

Figure 4.- Continued.

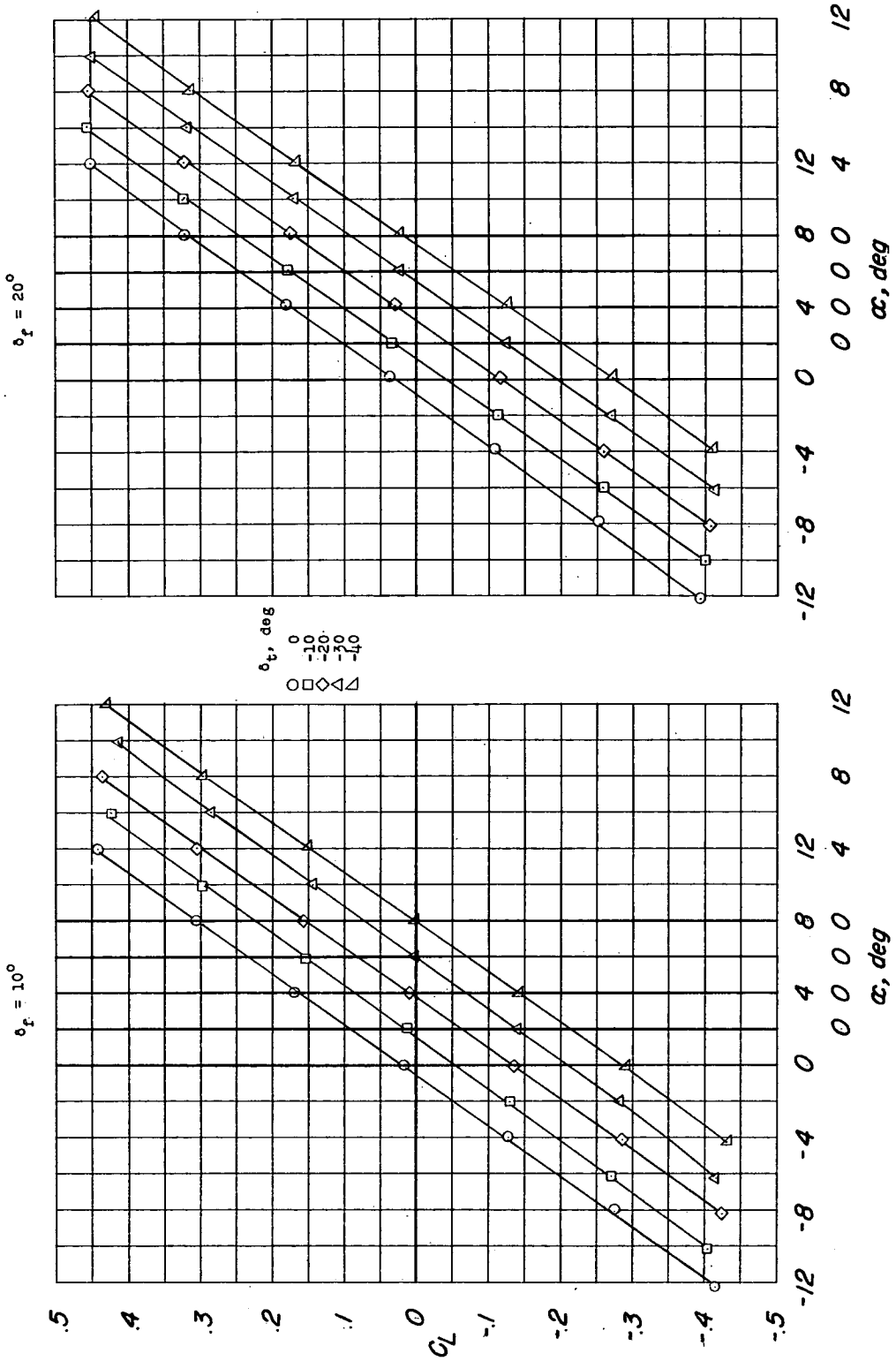

(b) Concluded.

Figure 4.- Continued.

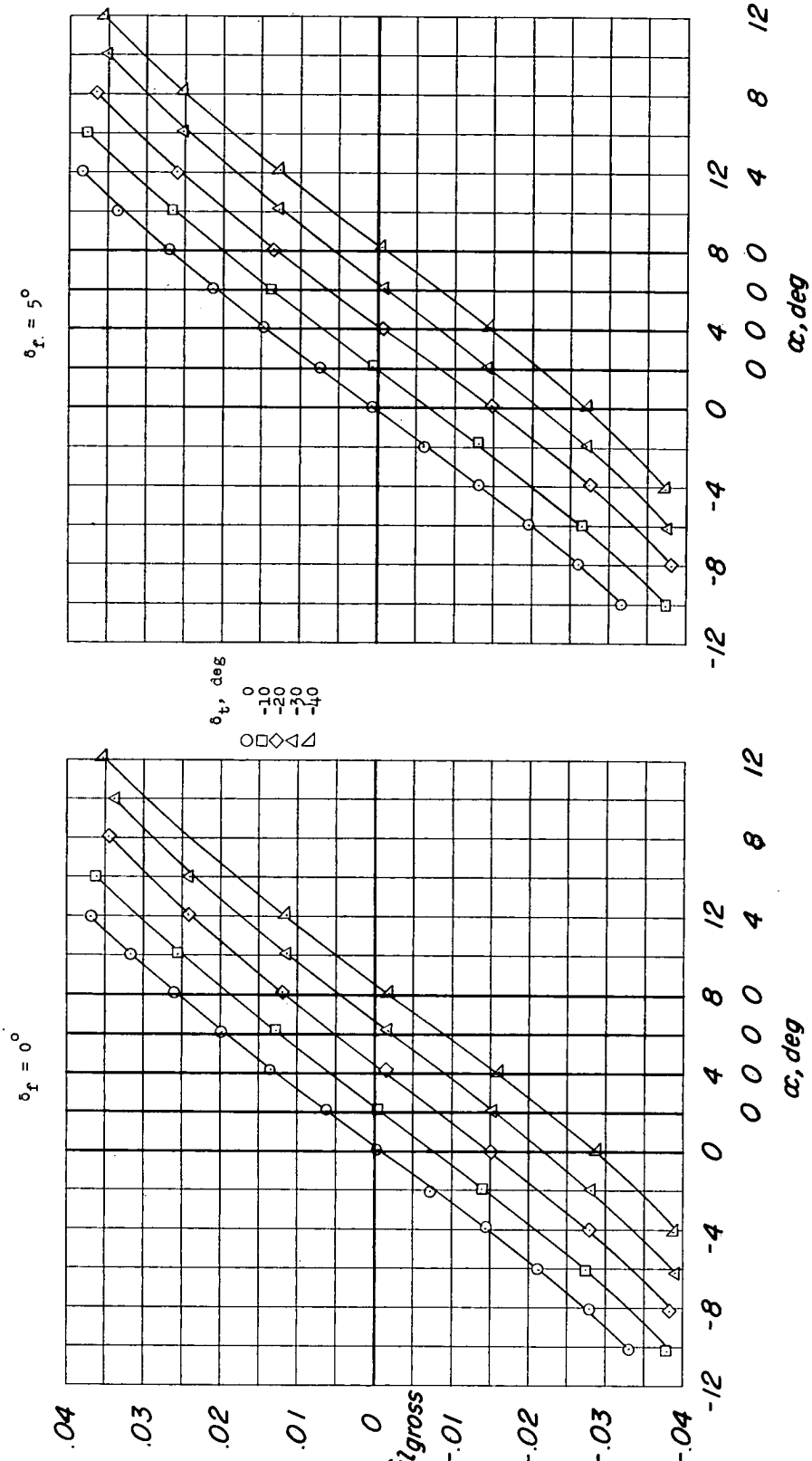

(c) $C_{l_{gross}}$ against α.

Figure 4.- Continued.

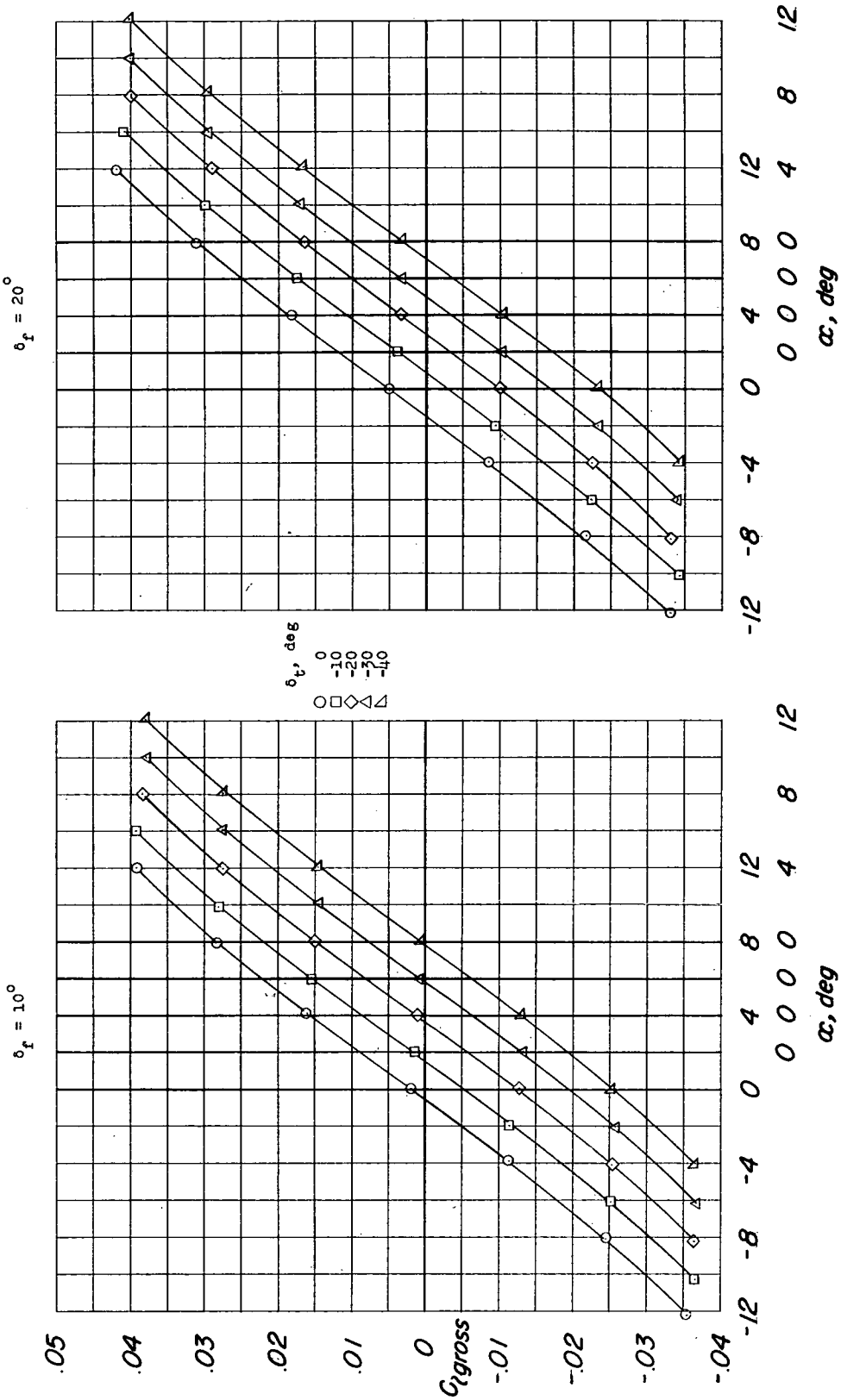

(c) Concluded.

Figure 4.- Concluded.

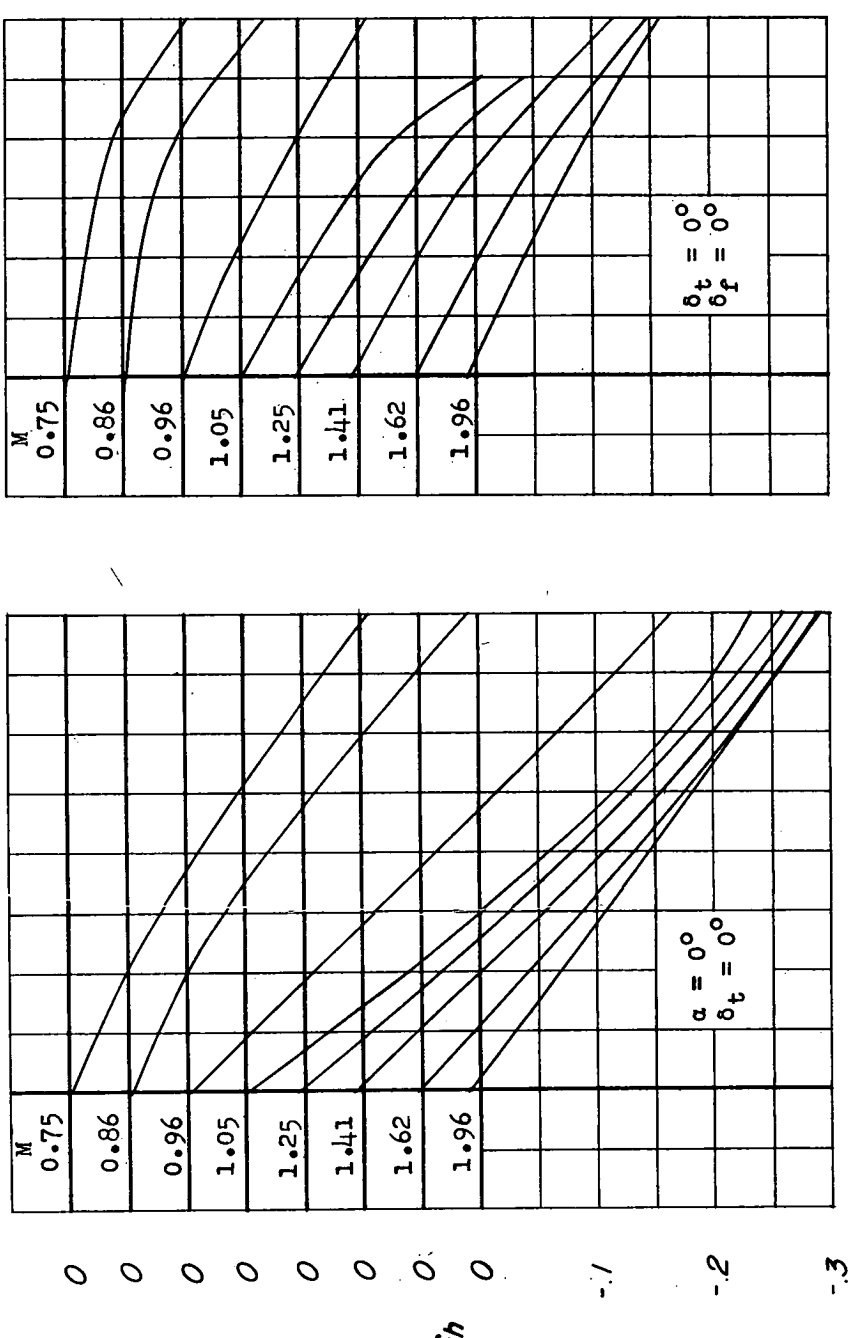

(a) C_h against δ_f.

(b) C_h against α.

Figure 5.- Variation of hinge-moment coefficient and rolling-moment coefficient with flap deflection and hinge-moment coefficient with angle of attack for various Mach numbers.

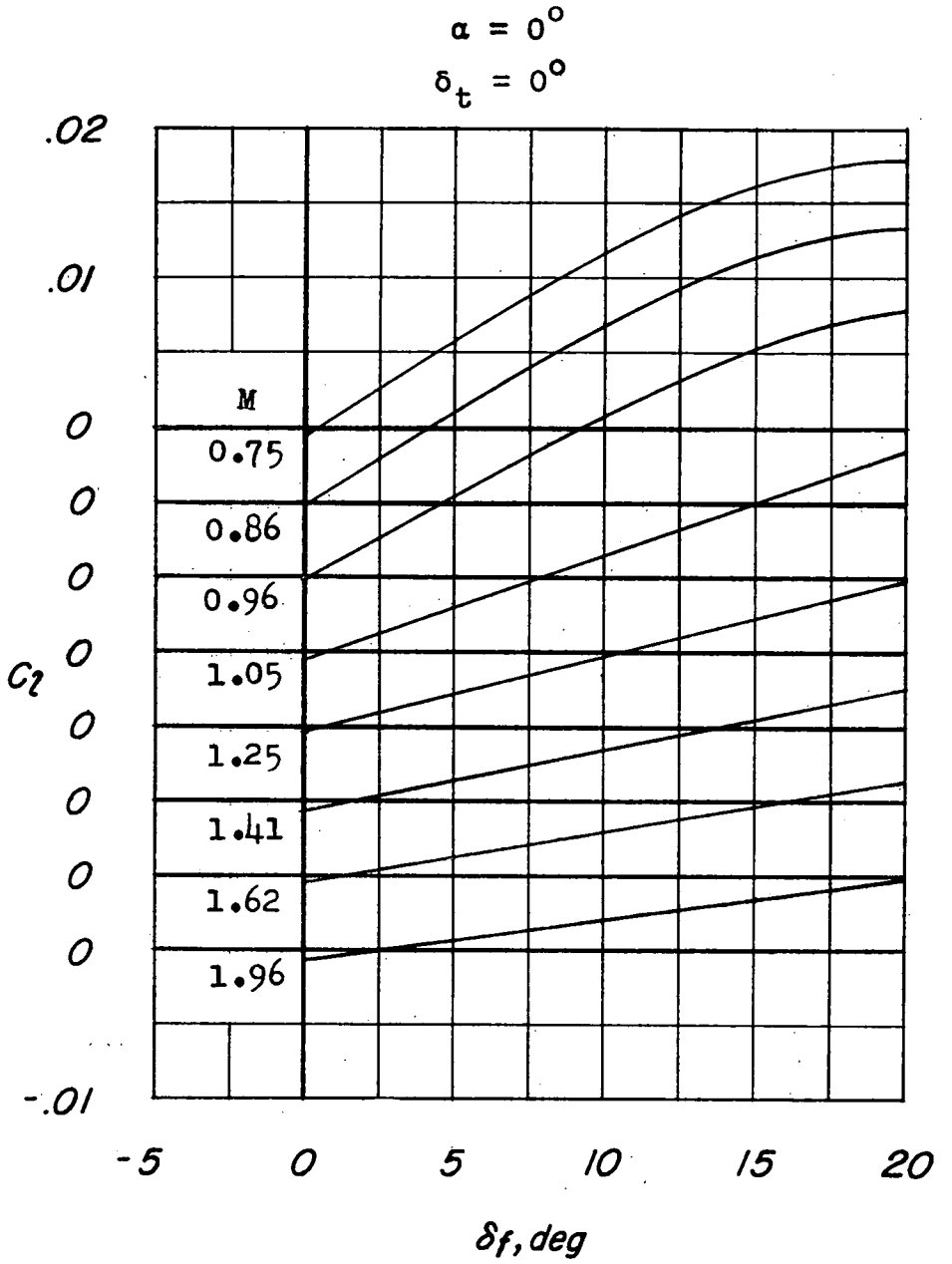

(c) C_l against δ_f.

Figure 5.- Concluded.

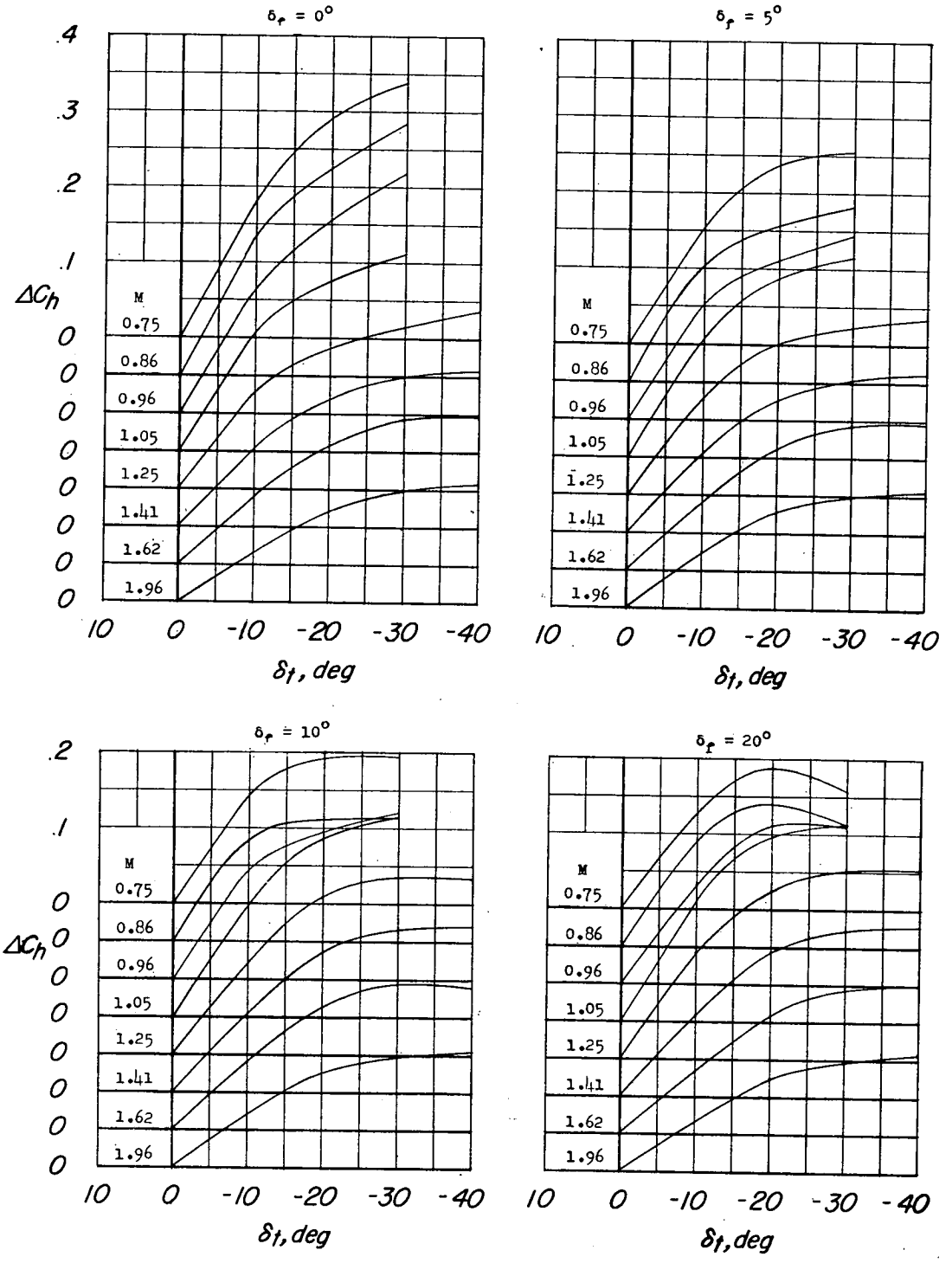

(a) ΔC_h against δ_t.

Figure 6.- Increment in hinge-moment coefficient and rolling-moment coefficient due to tab deflection plotted against tab deflection for various flap deflections and Mach numbers. $\alpha = 0°$.

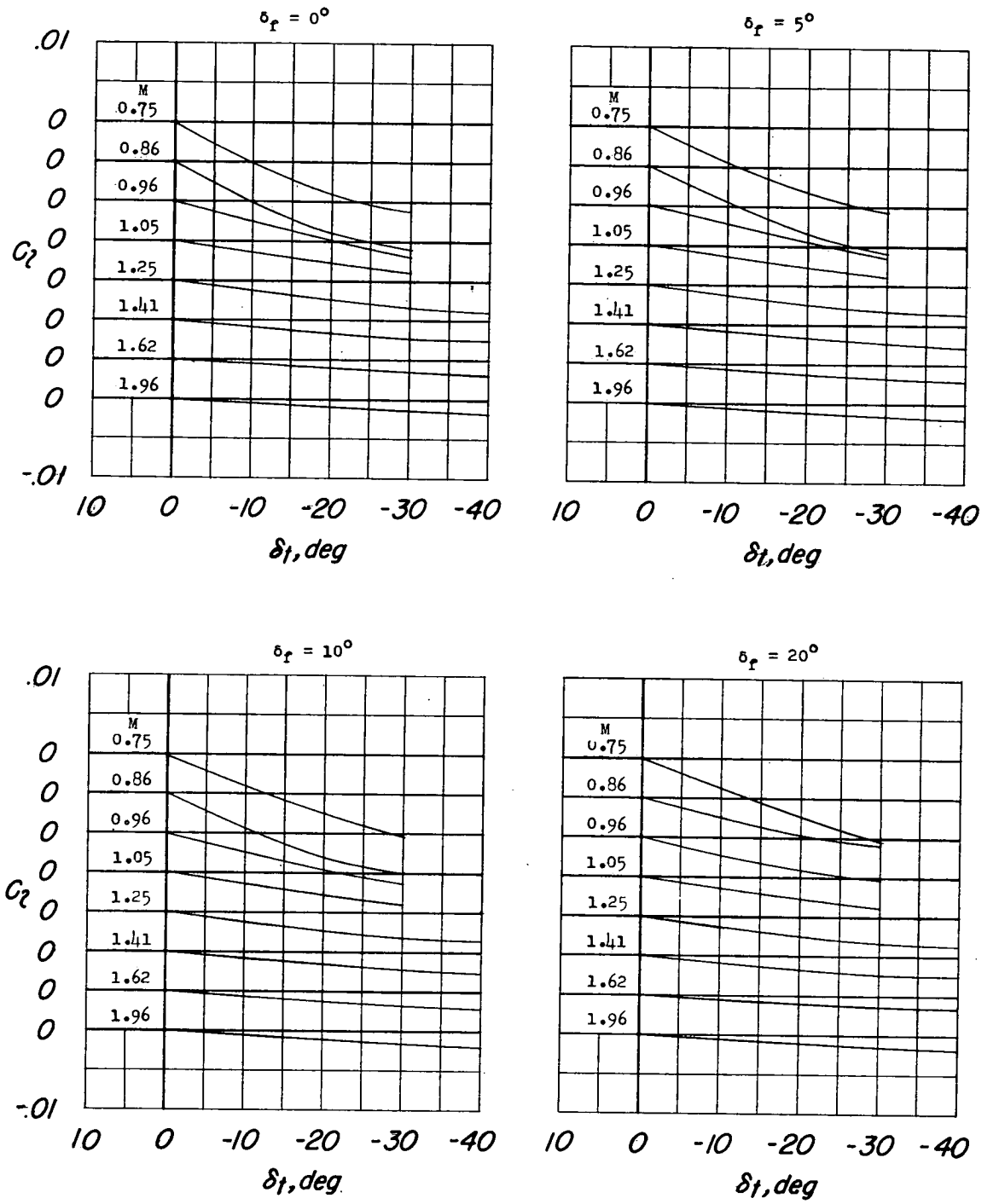

(b) C_l against δ_t.

Figure 6.- Concluded.

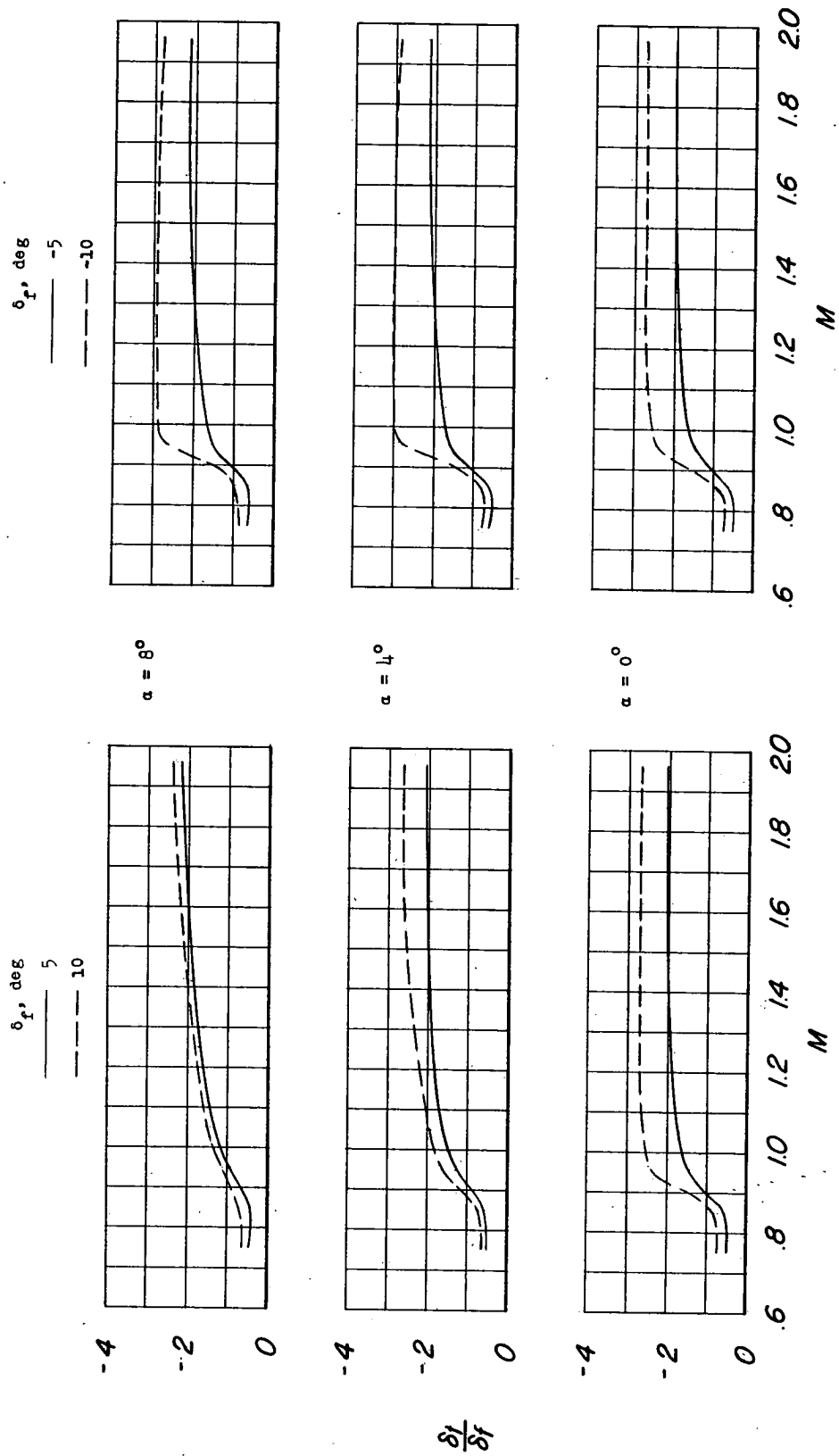

Figure 7.- Variation with Mach number of the ratio of tab deflection to flap deflection required for $\Delta C_h = 0$.

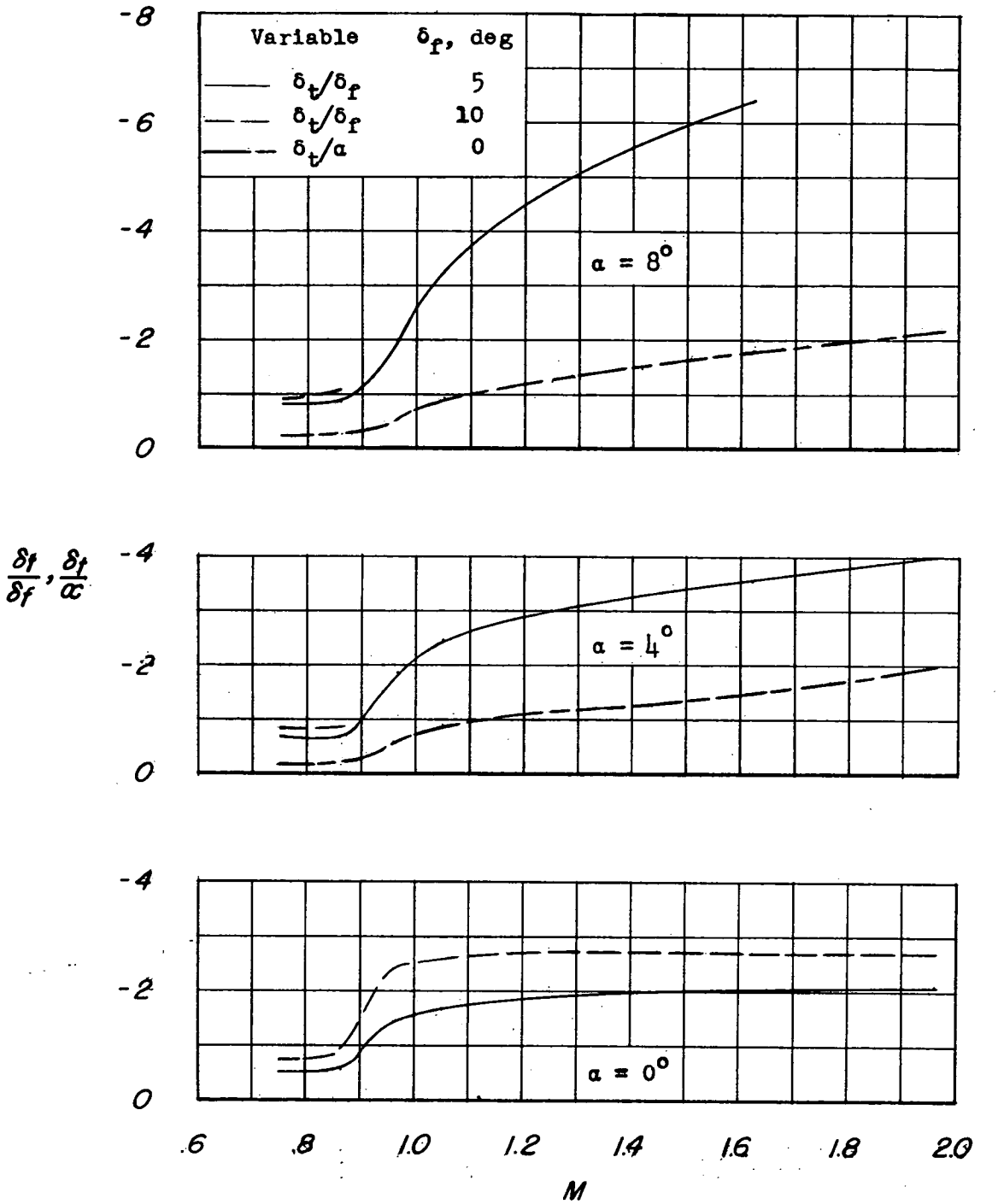

Figure 8.- Variation with Mach number of δ_t/δ_f and δ_t/α. $C_h = 0$.

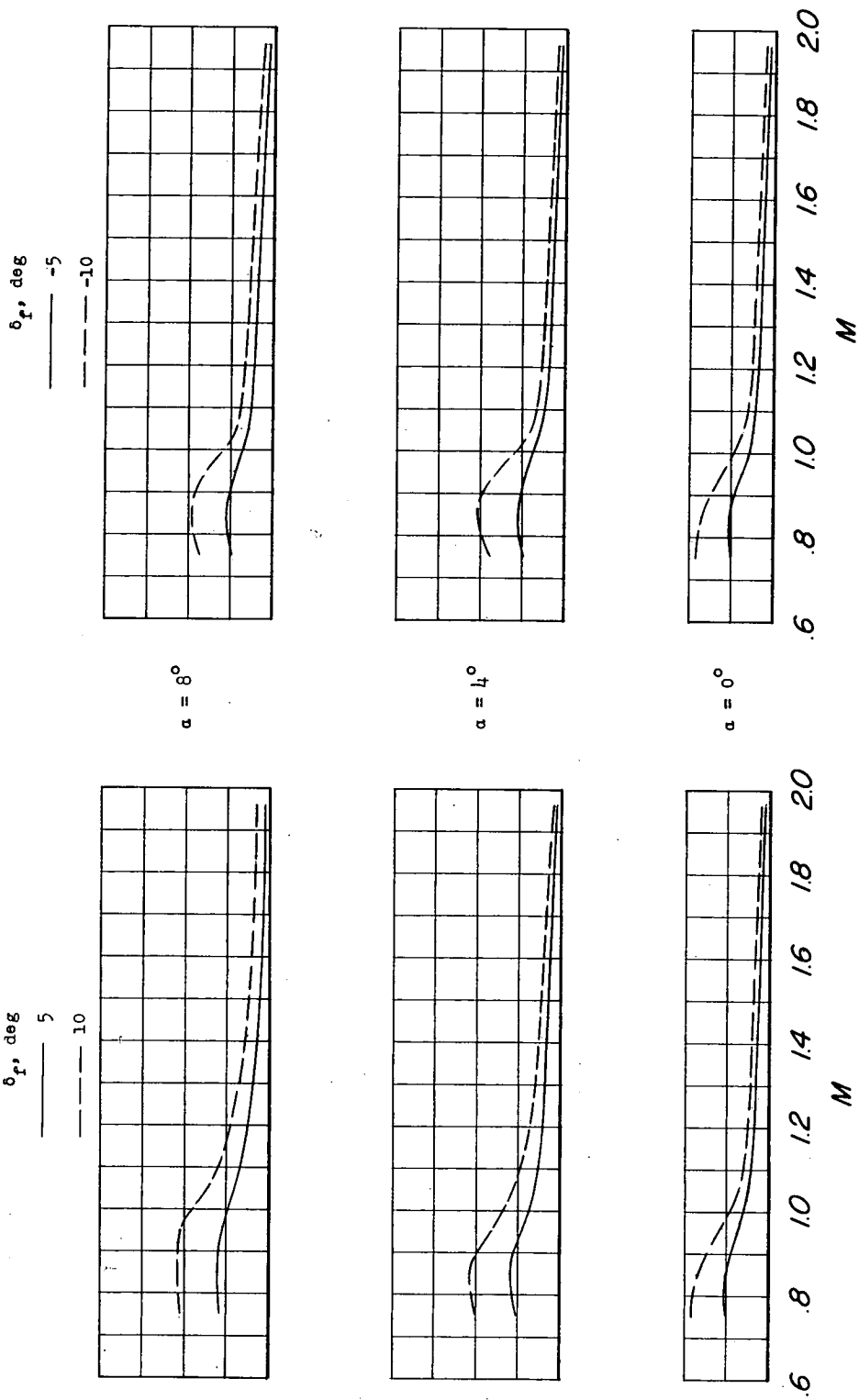

Figure 9.- Variation with Mach number of rolling-moment coefficient due to flap and tab deflection with tab deflected to give $\Delta C_h = 0$.

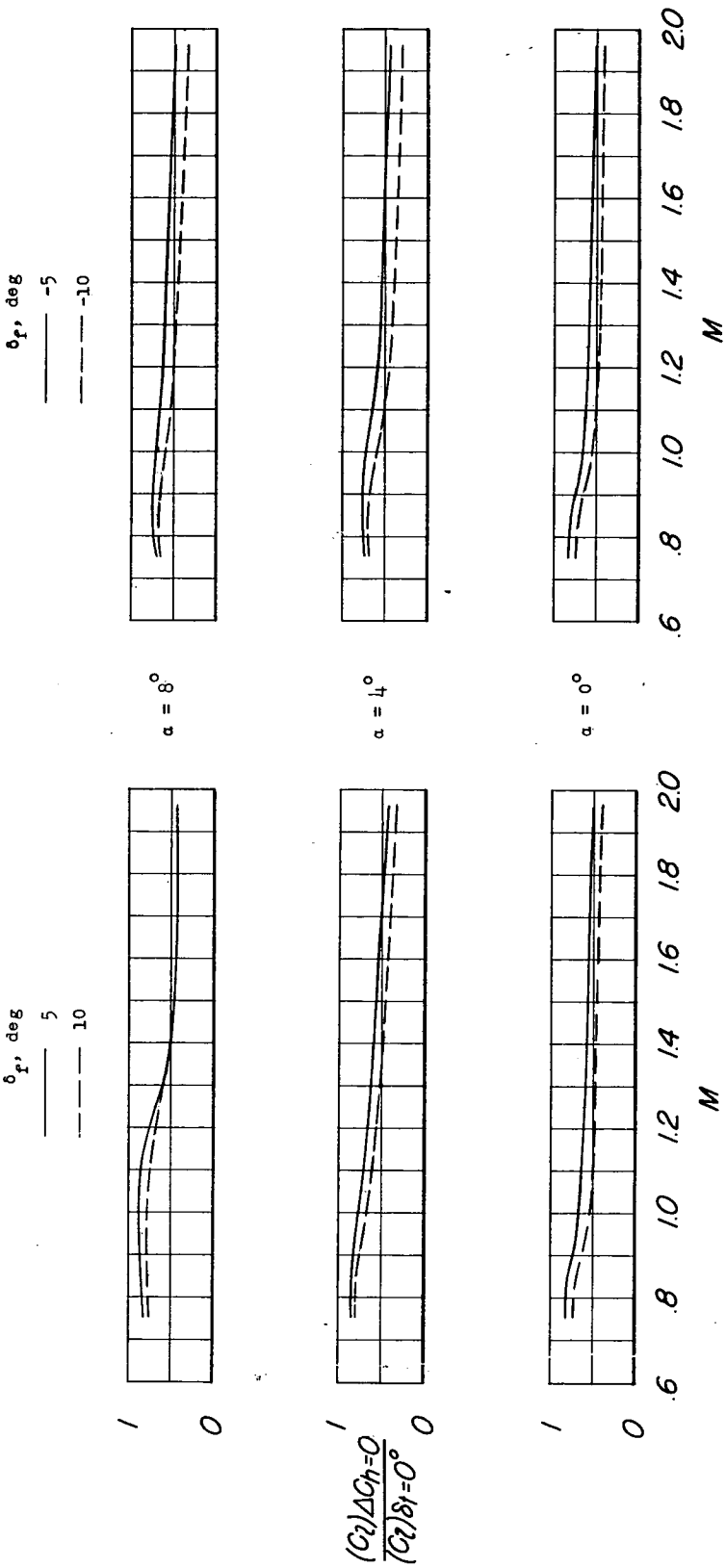

Figure 10.- Ratio of the rolling moment of the flap with the tab deflected to give $\Delta C_h = 0$ to that of the flap with the tab undeflected.

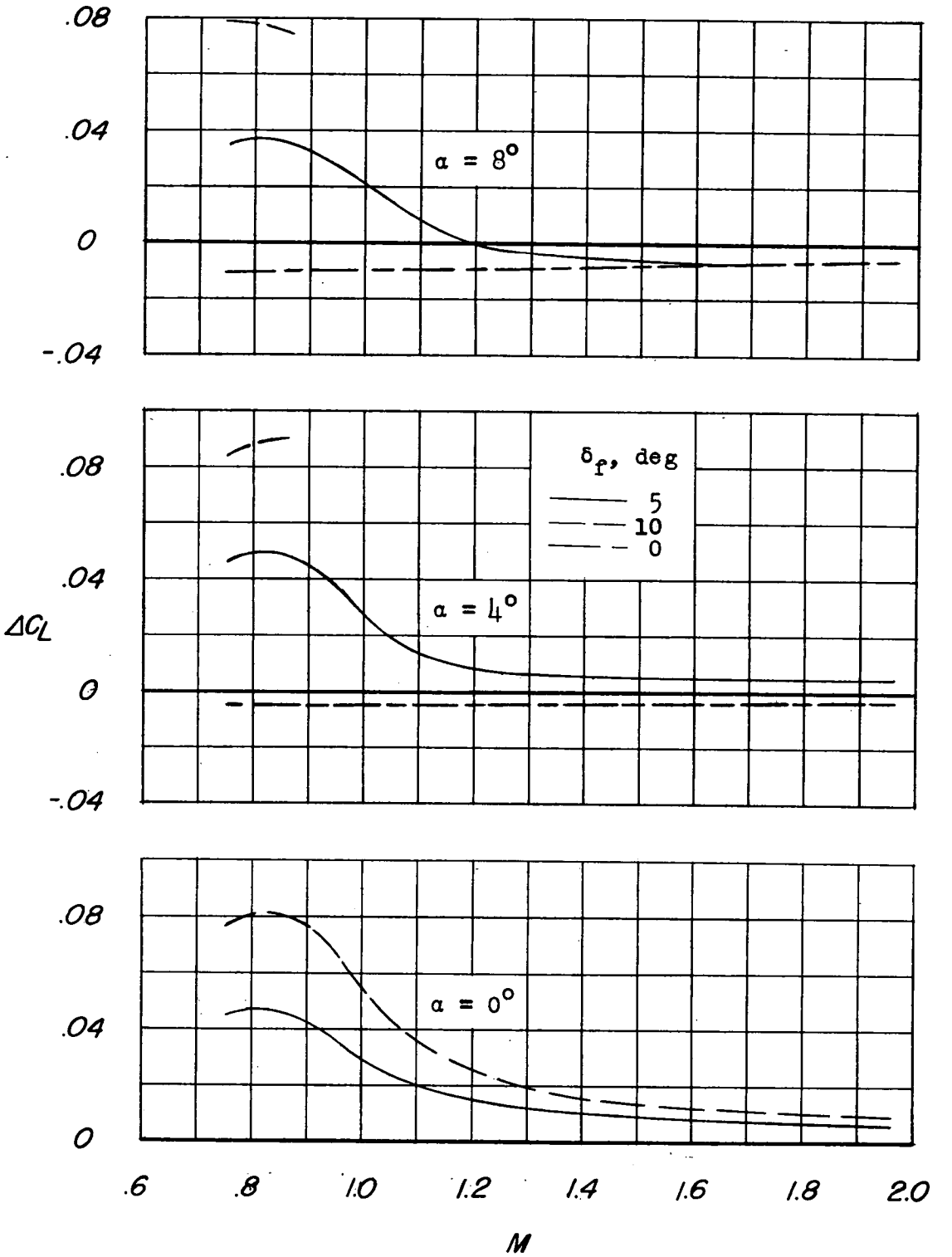

Figure 11.- Variation with Mach number of the increment in lift coefficient. $C_h = 0$.

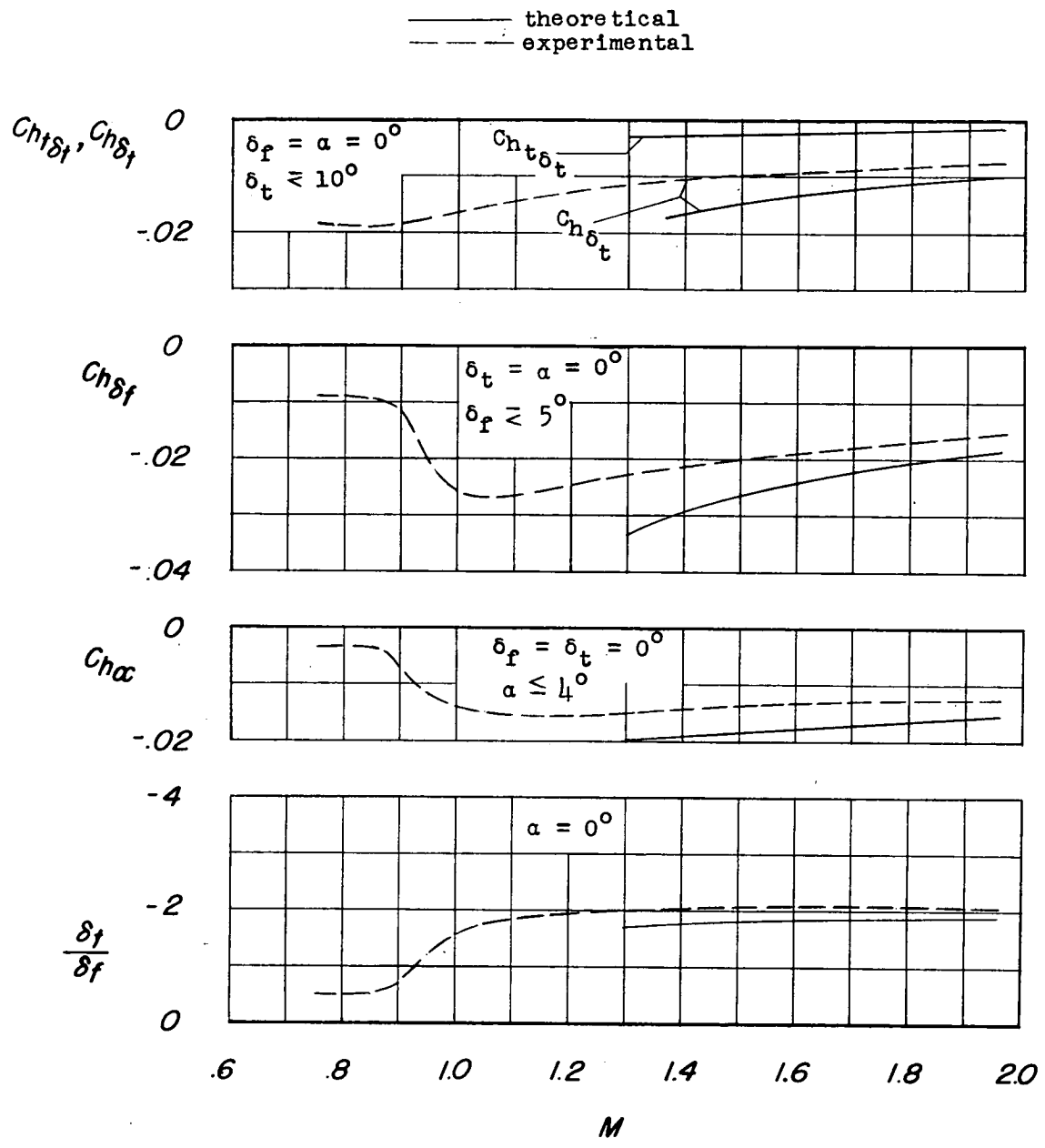

Figure 12.- Variation with Mach number of $C_{h_{t_{\delta_t}}}$, $C_{h_{\delta_t}}$, $C_{h_{\delta_f}}$, C_{h_α}, and δ_t/δ_f.

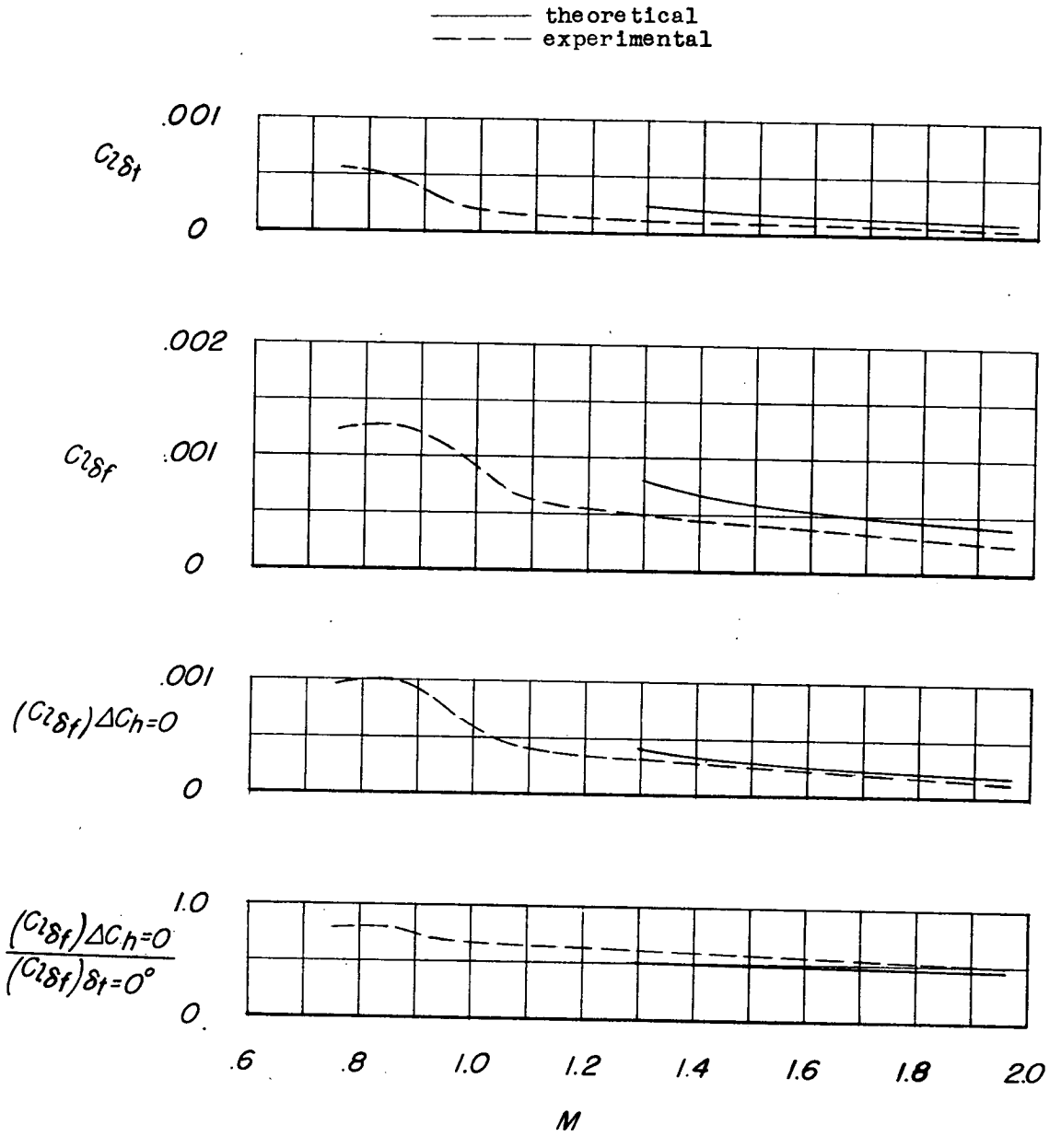

Figure 13.- Variation with Mach number of some flap and tab rolling-moment effectiveness parameters. $\alpha = 0^\circ$.

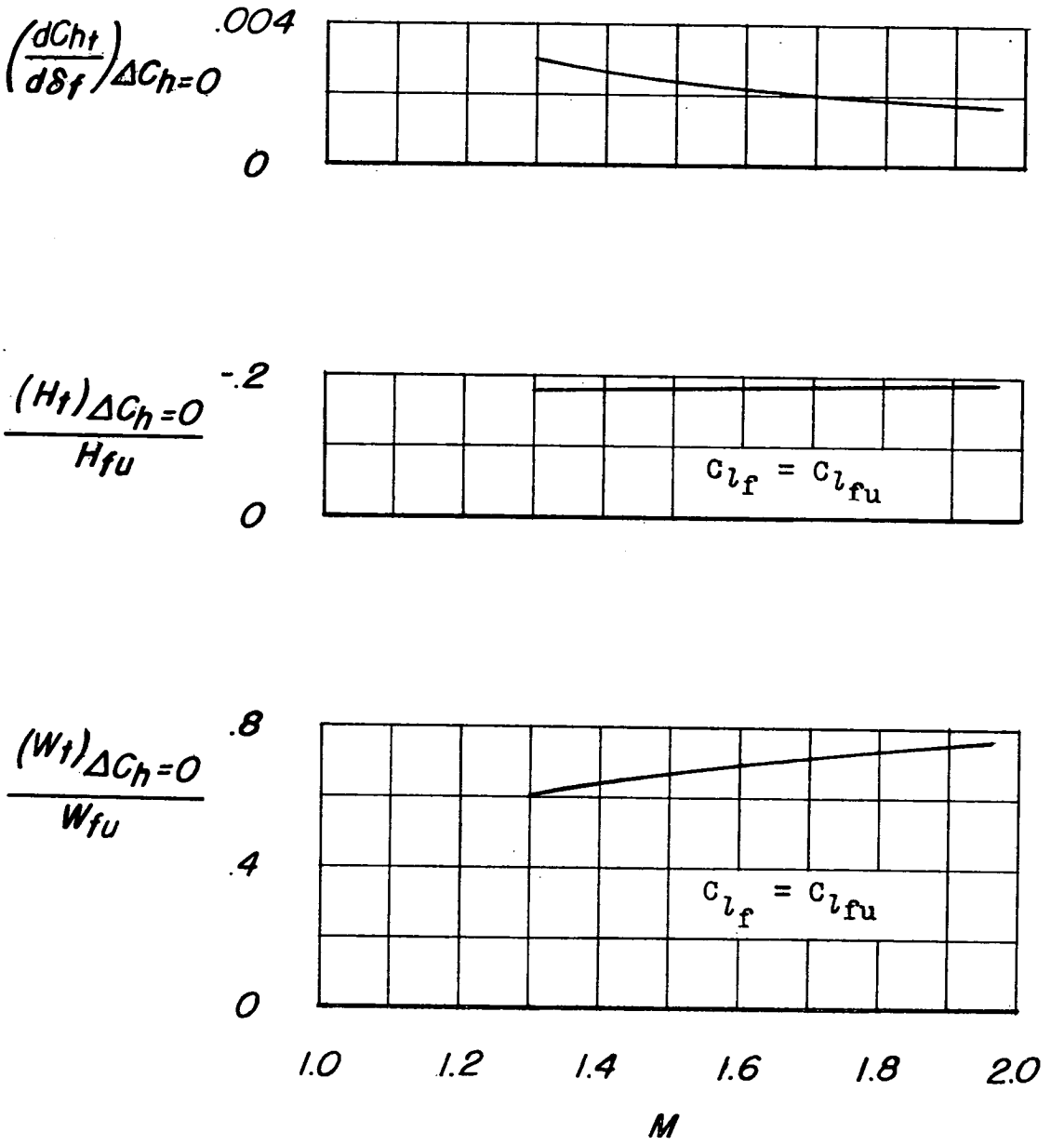

Figure 14.- Comparison of theoretical hinge-moment characteristics for a tabbed flap and an untabbed flap. $\alpha = 0^{\circ}$.